# ХИМИЧЕСКАЯ ИНФОРМАТИКА: ДОПОЛНИТЕЛЬНЫЕ ГЛАВЫ

**Лекция 8**

Информатика материалов
(первая лекция)

# МНОГООБРАЗИЕ ЗАДАЧ И ОБЪЕКТОВ

# MATERIALS FINGERPRINTS

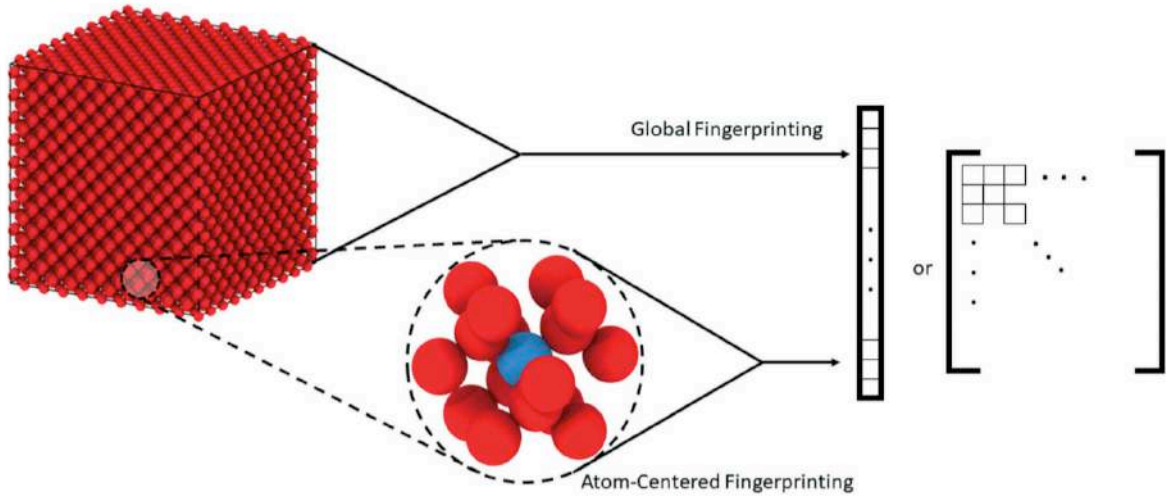


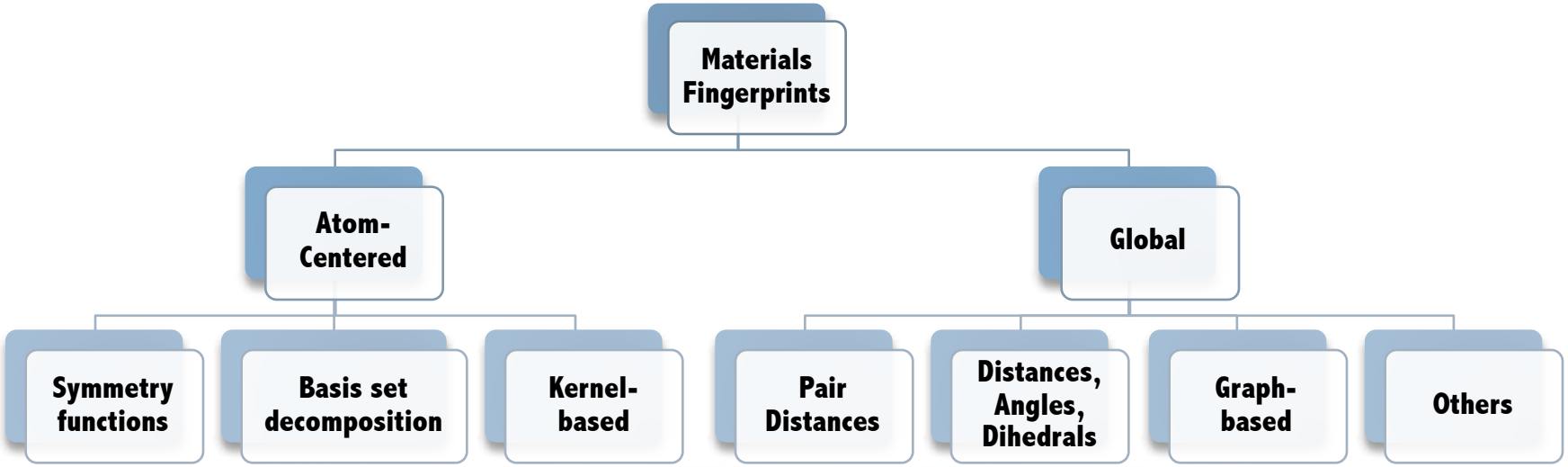


Reveil et al Classification of spatially resolved molecular fingerprints for machine learning applications and development of a codebase for their implementation Mol Syst Des & Engin (2018)

# ATOM-CENTERED SYMMETRY FUNCTIONS

Отпечатки, основанные на определении функции симметрии базируются на суммировании по связям и углам для всех атомов в пределах заданного радиуса

**Атомно-центрированные функции симметрии (ACSFs): Behler and Parinello**

$$G_i^{rad} = \sum_{j \neq i}^{N} e^{-\eta(r_{ij}-\mu)^2} f_c(r_{ij})$$

$$f_c(r_{ij}) = \begin{cases} \frac{1}{2}\left[\cos\left(\frac{\pi r_{ij}}{r_c}\right) + 1\right], r_{ij} \leq r_c \\ 0, r_{ij} \geq r_c \end{cases}$$

$$G_i^{ang} = 2^{1-\zeta} \sum_{j \neq i}^{N} \sum_{k \neq i,j}^{N} (1 + \lambda \cos\Theta_{ijk})^{\zeta} e^{-\eta(r_{ij}-\mu)^2} e^{-\eta(r_{ik}-\mu)^2} e^{-\eta(r_{jk}-\mu)^2} f_{ij} f_{ik} f_{jk}$$

$G_i^{rad}$ and $G_i^{ang}$ - atom-centered function

$r_{ij}$ - distances to all atoms j within a cutoff radius $r_c$

$\eta$ and $\mu$ - width and center of Gaussians (empirically defined)

$f_c$ - cutoff function (smoothing impact as a function of distance)

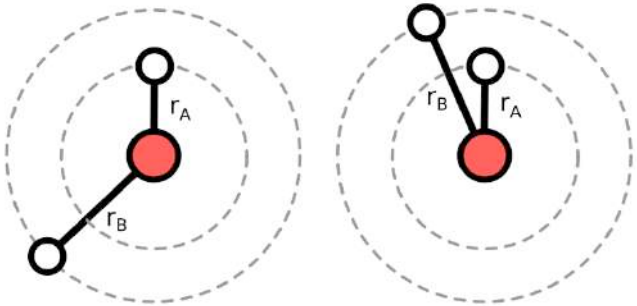


**Limitation: Empirical parametrization of symmetry functions**


Reveil et al **Classification of spatially resolved molecular fingerprints for machine learning applications and development of a codebase for their implementation** Mol Syst Des & Engin (2018)

Behler et al **Generalized Neural-Network Representation of High-Dimensional Potential-Energy Surfaces** Phys. Rev. Lett. 98, 146401

# ATOM-CENTERED SYMMETRY FUNCTIONS

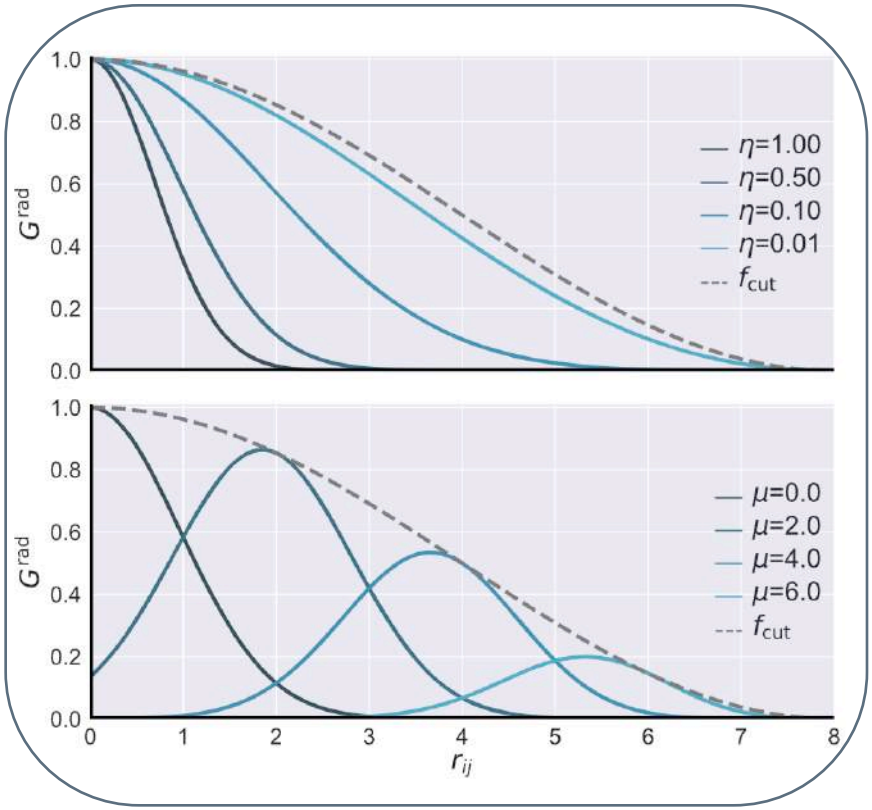


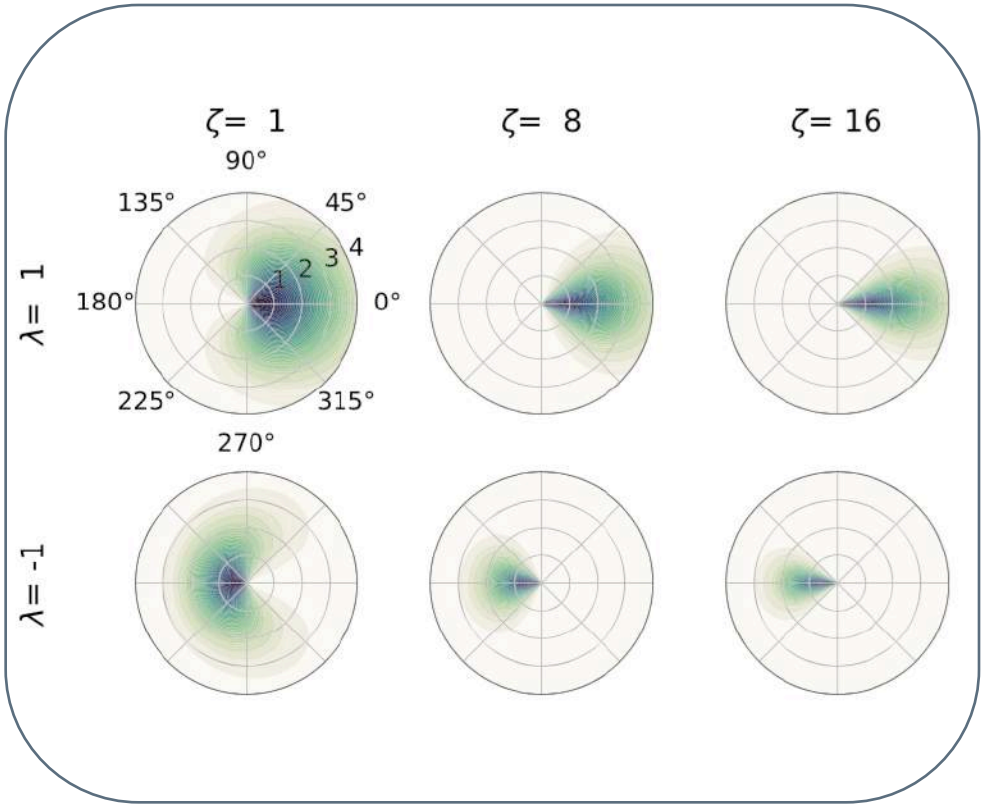


Reveil et al **Classification of spatially resolved molecular fingerprints for machine learning applications and development of a codebase for their implementation** Mol Syst Des & Engin (2018)

Behler et al **Generalized Neural-Network Representation of High-Dimensional Potential-Energy Surfaces** Phys. Rev. Lett. 98, 146401

# BISPECTRUM FINGERPRINTS

$$\rho_i(r) = \delta(r) + \sum_j \delta(1 - r_{ij}) f_c(|r_{ij}|) \qquad \text{where } f_c(r_{ij}) = \begin{cases} \frac{1}{2}\left[\cos\left(\frac{\pi r_{ij}}{r_c}\right) + 1\right], r_{ij} \le r_c \\ 0, r_{ij} \ge r_c \end{cases}$$

In order to achieve rotational invariance the spherical coordinates can be used.
Bispectrum – three-point correlation function that can be used to describe the atomic neighborhood

Atomic density is projected onto the surface of the four-dimensional unit sphere:

$$r \equiv \begin{pmatrix} x \\ y \\ z \end{pmatrix} \longrightarrow \begin{array}{c} \phi = \arctan(\frac{y}{x}) \\ \theta = arccos(z/|r|) \\ \theta_0 = \pi|r|/r_0 \end{array}$$

where $\phi, \theta, \theta_0 - \text{polar angles};$
$r_0 > r_{cut}/\pi$

4D spherical harmonics (Wigner matrices $U^j_{m'm}$) – complete basis for the interior of the 3D sphere

The projection of the atomic density on the surface of the 4D sphere can be represented through the set of the ordinary Clebsch-Gordon coefficients that are expansion coefficients of total angular momentum eigenstates:

$$c^j_{m'm} = \left\langle U^j_{m'm} | \rho \right\rangle$$

$$B_{j_1,j_2,j} = \sum_{m'_1, m_1=-j_1}^{j_1} \sum_{m'_2, m_2=-j_2}^{j_2} \sum_{m', m=-j}^{j} \left(c^j_{m'm}\right) c^{jm}_{j_1,m_1,j_2,m_2} \; c^{jm'}_{j_1,m'_1 j_2 m'_2} c^{j_1}_{m'_1 m_1} c^{j_2}_{m'_2 m_2}$$

Bartok et al **Gaussian Approximation Potentials: The Accuracy of Quantum Mechanics, without the Electrons** Phys Rev Lett (2010) 104, 136403

Bartok et al **On representing chemical environments** Phys Rev (2013) 87, 184115

# SMOOTH OVERLAP OF ATOMIC POSITIONS (SOAP) SIMILARITY KERNELS

Локальная атомная конфигурация $\widetilde{x_l}$ может быть выражена определена посредством сглаженных атомных плотностей, центрированных на атоме $l$:

$$\rho_i(r) = \sum_j \omega(z_i)\varphi_\sigma(r - r_{ij}) f_c(|r_{ij}|) \qquad \text{where } f_c(r_{ij}) = \begin{cases} \frac{1}{2}\left[\cos\left(\frac{\pi r_{ij}}{r_c}\right) + 1\right], r_{ij} \le r_c \\ 0, r_{ij} \ge r_c \end{cases}$$

$z_i$ — atomic number
$\omega_i$ — associated with given atomic type weight

Атомные плотности заданы посредством гауссовых функций с дисперсией $\sigma^2$

$$\varphi_\sigma(r) = exp(-r^2/2\sigma^2)$$

Определение ядра как перекрывания двух локальных атомных плотностей, интегрированное с учетом всех возможных трехмерных вращений и инвариантного по отношению к вращению:

$$S(\tilde{x}, \tilde{x}') = \int_{\mathbb{R}^3} \rho_{\tilde{x}}(r)\rho_{\tilde{x}'}(r)dr \qquad k(\tilde{x}, \tilde{x}') = \int_{SO(3)} S(R\tilde{x}, \tilde{x}')^p dR$$

Нормализованное ядро (кернел) с увеличением в областях наибольшего значения, принимаемого функцией при $\zeta > 1$:

$$\widetilde{K}(\tilde{x}, \tilde{x}') = \left[\frac{k(\tilde{x}, \tilde{x}')}{\sqrt{k(\tilde{x}, \tilde{x})k(\tilde{x}', \tilde{x}')}}\right]^\zeta$$

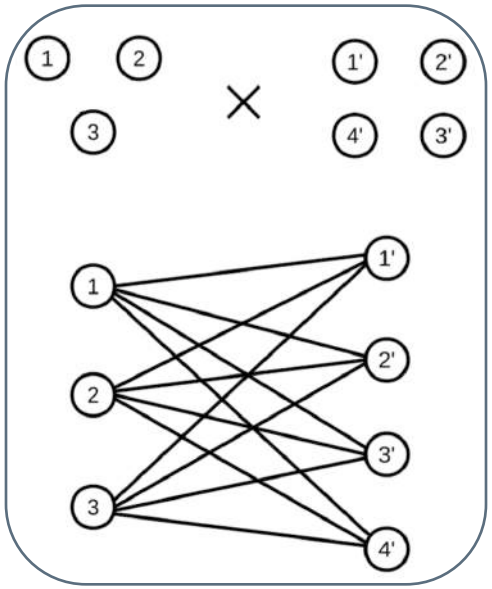


Graph interpretation of the SOAP kernel. Two local environments comprised of 3 and 4 atoms are compared by forming a bipartite graph that links pairs of atoms

Ferre et al **Learning molecular energies using localized graph kernels** J. Phys. Chem. (2017) 146, 114107

# STEINHARDT ORDER PARAMETERS

The complex vector $q_{lm}(i)$ of particle ***i*** is defined as follows:

$$q_{lm}(i) = \frac{1}{N_b(i)} \sum_{i=1}^{N_b(i)} Y_{lm}(r_{ij})$$

$Y_{lm}(r_{ij})$ – spherical harmonics

Steinhardt order parameters:

$$q_l(i) = \sqrt{\frac{4\pi}{2l+1} \sum_{m=-l}^{l} |q_{lm}(i)|^2}$$

$$S_{ij} = \sum_{m=-6}^{6} q_{6m}(i) q_{6m}^*(i)$$

Two particles are connected if $\boldsymbol{S_{ij}}$ >0.5
A particle is solidlike if $\boldsymbol{N_{connect}}$ > 6, otherwise - liquidlike

Lechner et al **Accurate determination of crystal structures based on averaged local bond order parameters** J Chem Phys (2008) 129, 114707

# MORTON SPACE-FILLING CURVES

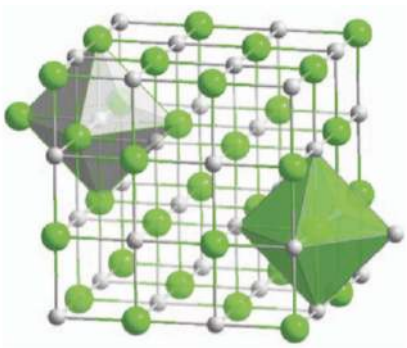

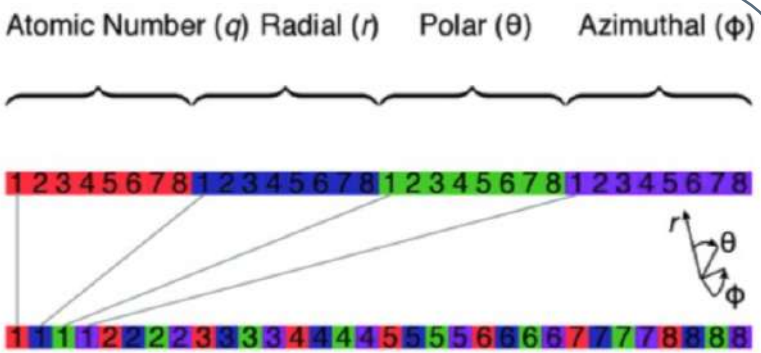


**Atomic layer:**
Atomic number
Atomic and coordination number
Coulomb matrix

$$c = \sum_{i=1}^{N_\beta} \frac{Z_\alpha Z_\beta}{r_\alpha \beta_i}$$

**Basic steps:**

- Orientation along the principal moments of inertia
- Cartesian to spherical coordinates mapping
- Four-dimensional grid formation
- Compressing to one-dimensional vector

Jasrasaria et al **Space-Filling Curves as a Novel Crystal Structure Representation for Machine Learning Models** Arxiv (2016)

# ФРАГМЕНТНЫЕ ДЕСКРИПТОРЫ ДЛЯ ПРОГНОЗИРОВАНИЯ СВОЙСТВ НЕОРГАНИЧЕСКИХ КРИСТАЛЛИЧЕСКИХ СОЕДИНЕНИЙ

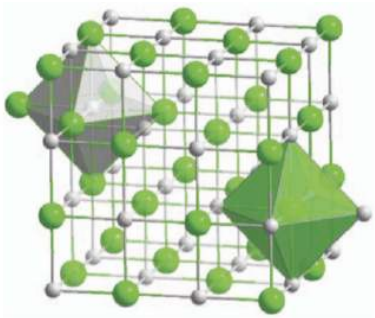

Структурный тип

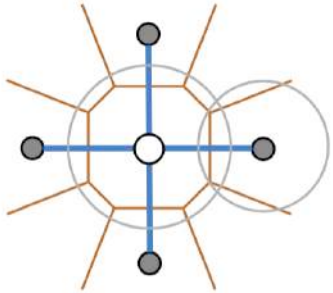

Полиэдр Вороного-Дирихле

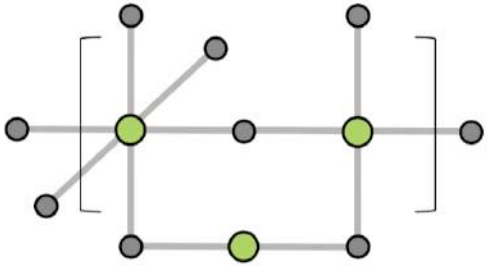

Генерация графа, ассоциирование вершин графа со значением выбранных ключевых параметров, описывающих свойства образующих его химических элементов

Генерация фрагментов

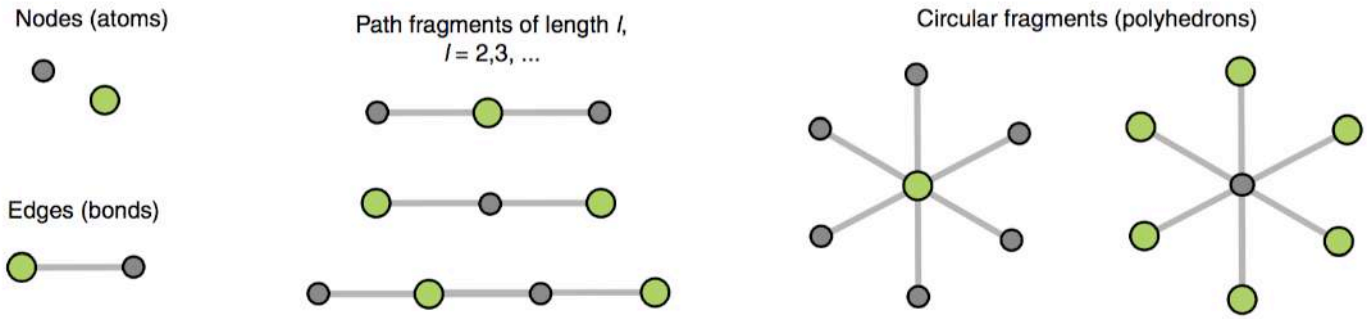


$$T^{E} = \sum_{i=1}^{n-1} \sum_{j=i+1}^{n} |q_i - q_j| M_{ij} \qquad T^{E}_{bond} = \sum_{\{i,j\} \in bonds} |q_i - q_j| M_{ij}$$

Isayev et al **Universal fragment descriptors for predicting properties of inorganic crystals** Nature Commun. 2017; 8: 15679

# КОРРЕЛИРОВАННЫЙ БЕСПОРЯДОК

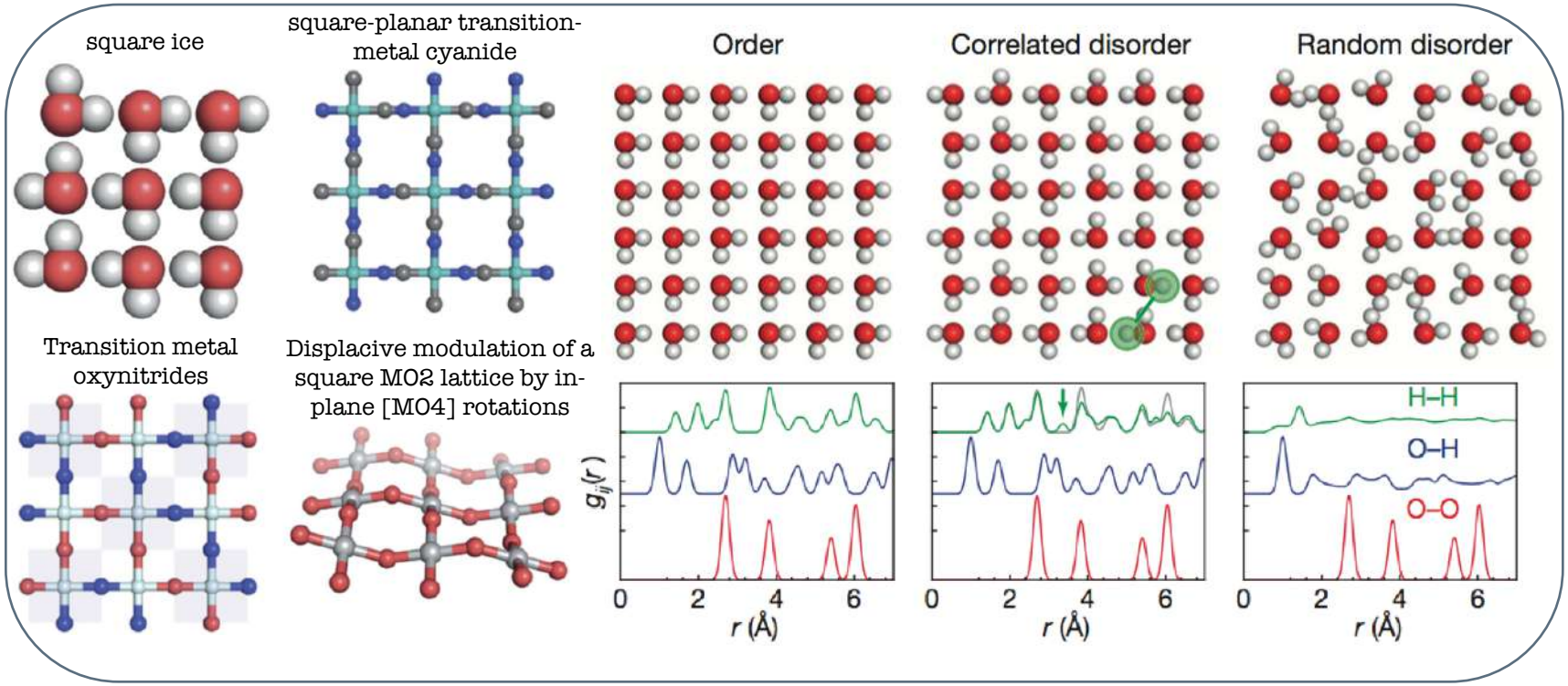


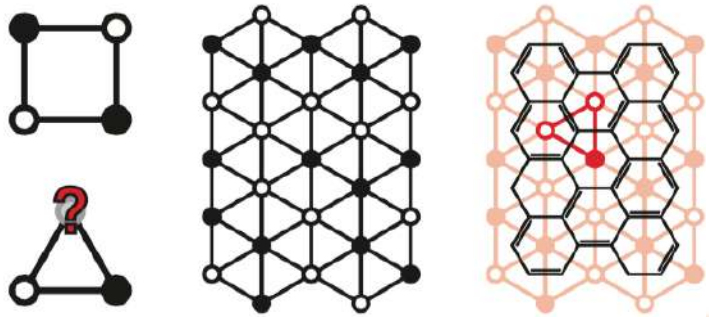

$$S_{\text{config}} \simeq R \ln\left(\frac{n}{2^{d/2}}\right)$$

Число Полинга P= $\left(\frac{n}{2^{d/2}}\right)$

(склонность системы к беспорядку)

Overy et al Design of crystal-like aperiodic solids with selective disorder–phonon coupling (2016) Nature Comm 7:10445

Keen, D. A. & Goodwin, A. L. The crystallography of correlated disorder. Nature 521, 303–309 (2015).

# COMMON NEIGHBOR ANALYSIS: SIGNATURE

Controlling microscopic nature:

- Nanoscale colloidal crystals
- Micro-sized colloids

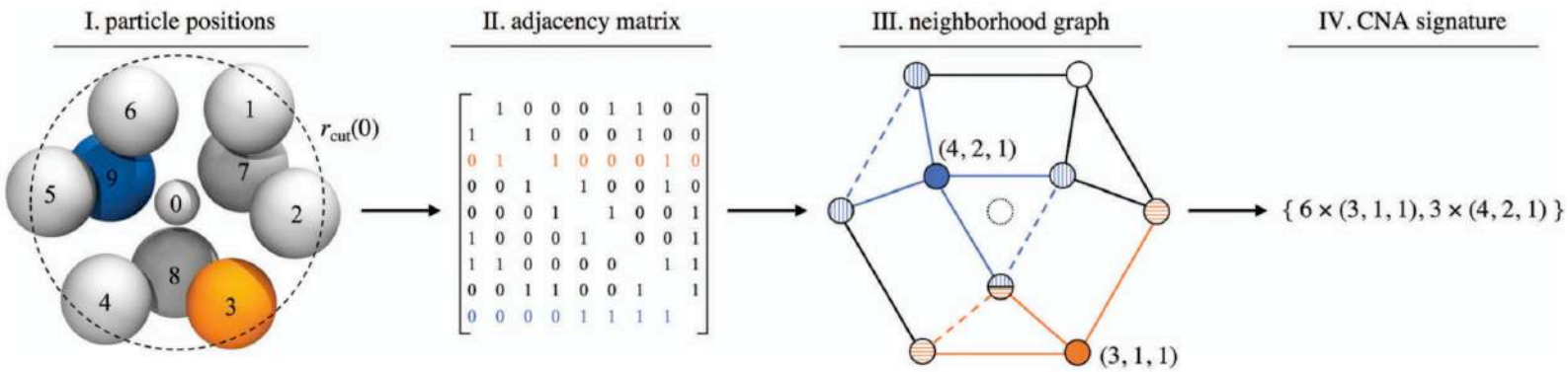


$r_{cut}$ – empirical parameter

CNA signature:
Number of adjacent nodes
Number of edges between those nodes
Length of the longest path among only those edges

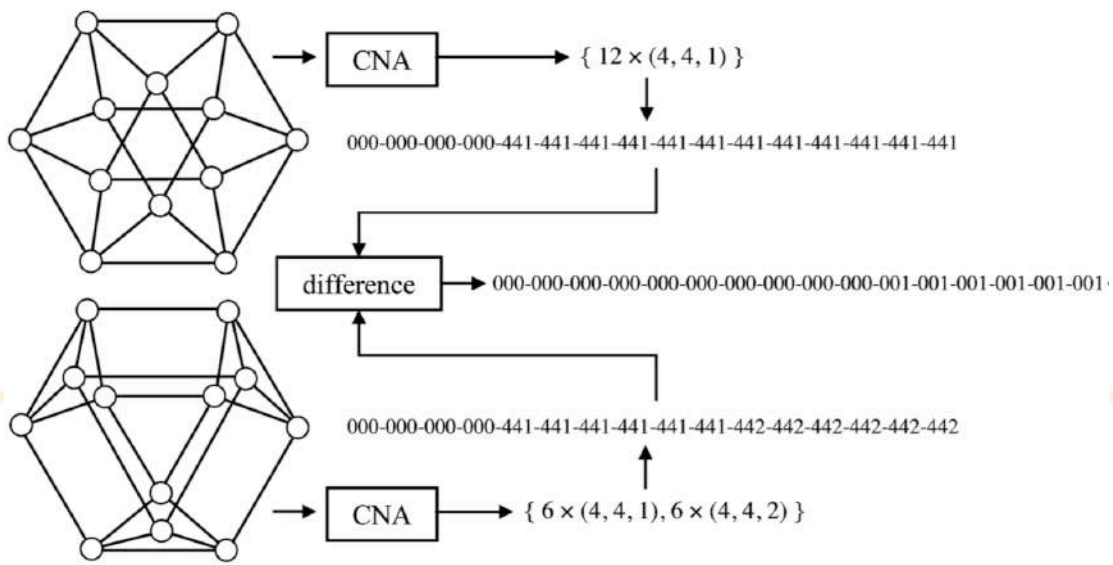

# ФРАГМЕНТНЫЕ ДЕСКРИПТОРЫ ДЛЯ ПРОГНОЗИРОВАНИЯ СВОЙСТВ НЕОРГАНИЧЕСКИХ КРИСТАЛЛИЧЕСКИХ СОЕДИНЕНИЙ

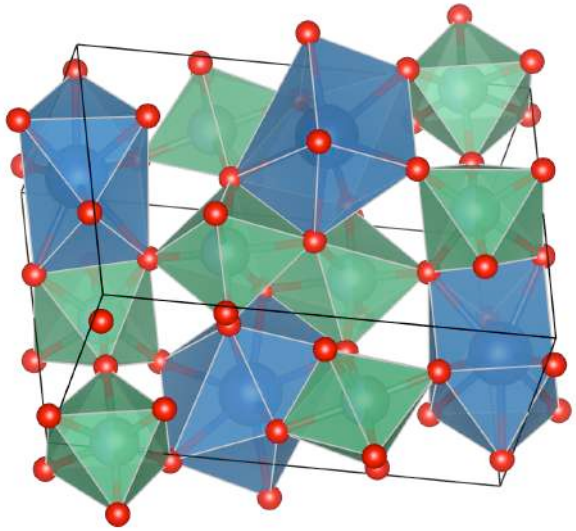

Aeschynite $A^{3+}B^{4+}C^{5+}O_6$ (SG: *Pnma*)
A=RE(57-63), B=$Ti^{4+}$, C=TM

Structure parameter

P = $m \cdot n/2^d$

*m* – relative number of polyhedra connected similarly
*n* – order of the point group symmetry
*d* – connectivity type (nodes, edges, grains)

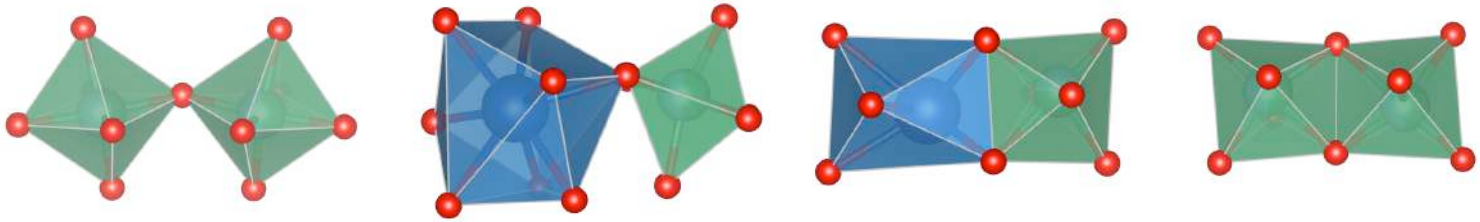

$$P = \sum_i m_i \cdot n_i/2^d$$

# ELECTRONIC FINGERPRINTS

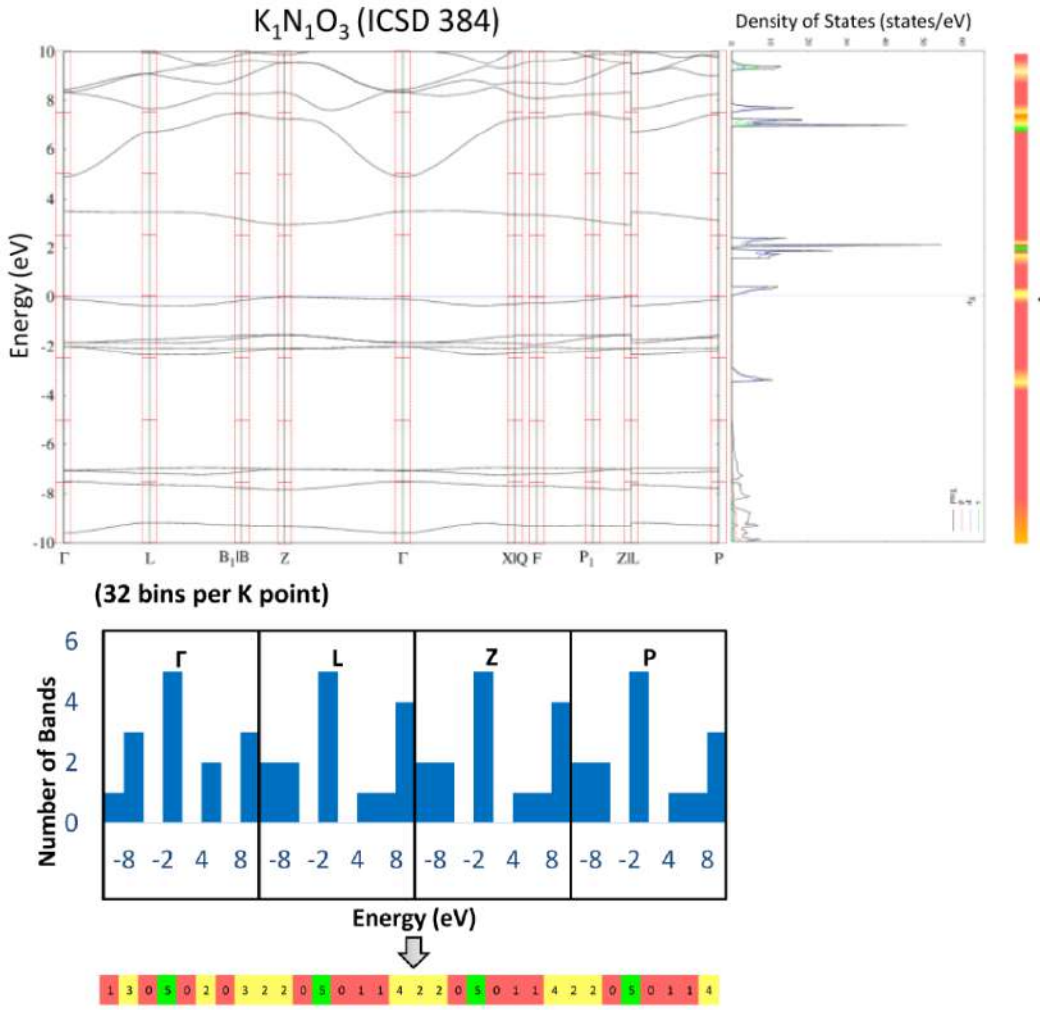


Isayev et al **Materials Cartography: Representing and Mining Materials Space Using Structural and Electronic Fingerprints** Chem Mater (2015) 27,735

# СКРИНИНГ СОЕДИНЕНИЙ С ЗАДАННЫМИ СВОЙСТВАМИ

# MATERIALS CARTOGRAPHY: REPRESENTING AND MINING MATERIALS SPACE FOR SCREENING OF MATERIALS WITH TARGET PROPERTIES

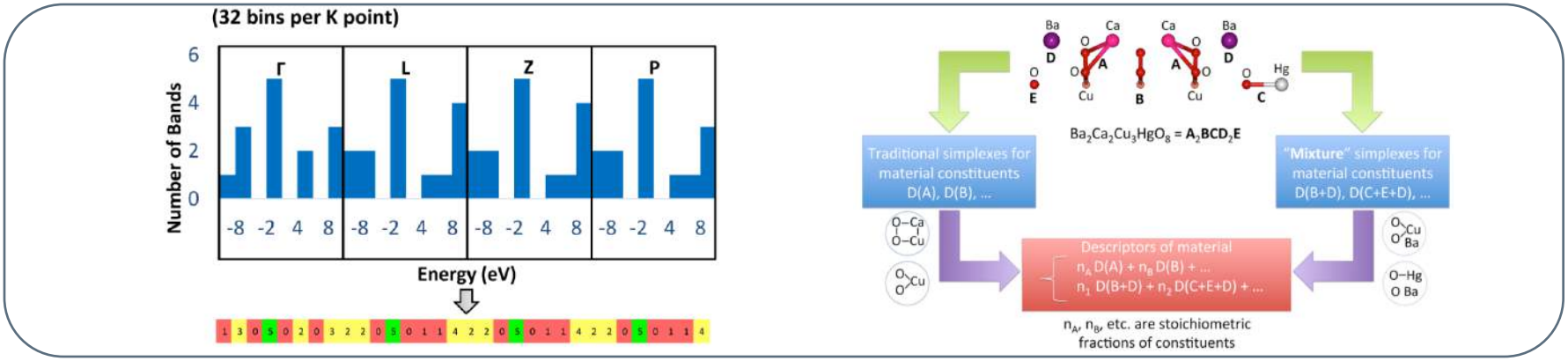


**Network representation:**

- Gephi package
- ForceAtlas algorithm

**Data:**

- Handbook of Superconductivity
- Handbook of Chemistry and Physics
- SuperCon Database

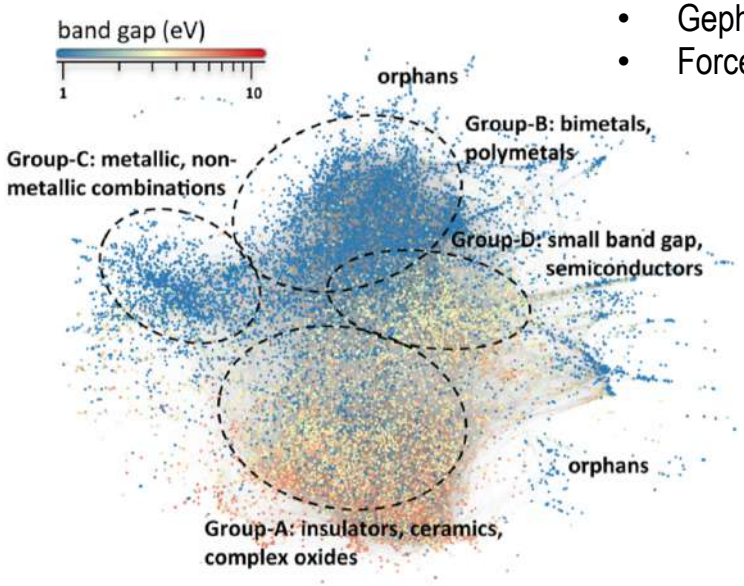


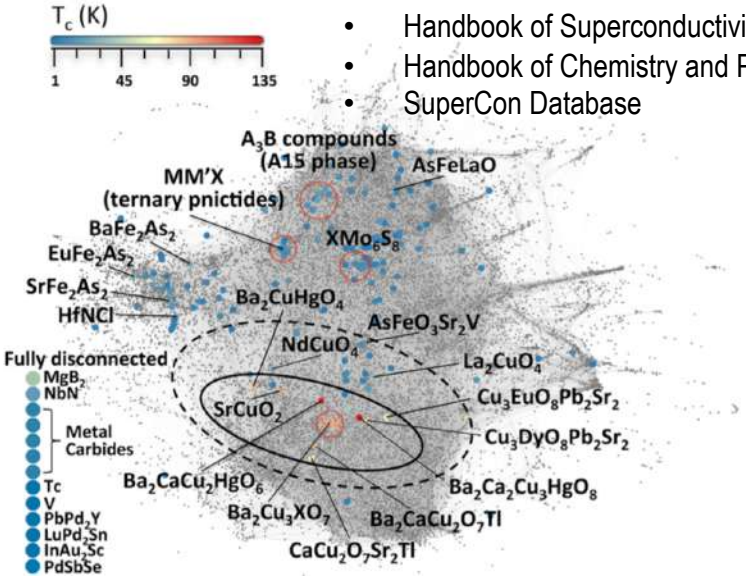


Isayev et al **Materials Cartography: Representing and Mining Materials Space Using Structural and Electronic Fingerprints** Chem Mater (2015) 27,735

# ПРОГНОЗИРОВАНИЕ СТРУКТУРЫ

# ПРОГНОЗИРОВАНИЕ СТРУКТУРЫ

Experimental data

Compound = $x_A x_B$

$x_A$=1 -> SG1
$x_A$=0.75 -> SG2
$x_A$=0.5 -> SG3
$x_A$=0.25 -> ?
$x_A$=0 -> SG4

Database search

$x_A$=0.25

List of candidate types of crystal structures or SGs

SG6 (17)
SG7 (9)
SG8 (8)
SG9 (5)
SG10 (2)
SG5 (2)
…

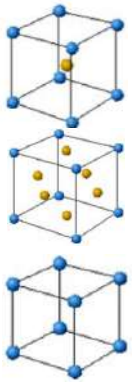

*Ab initio* formation enthalpy values

$$p(\mathbf{X}) = \frac{1}{Z}\prod_i p(x_i)\prod_{j<k} g^{(2)}(x_j, x_k)$$

$$g^{(2)}(x_i, x_j) = \frac{p(x_i, x_j)}{p(x_i)p(x_j)}$$

Cumulative function *g* – correction term for using the information from the compounds with correlated behavior

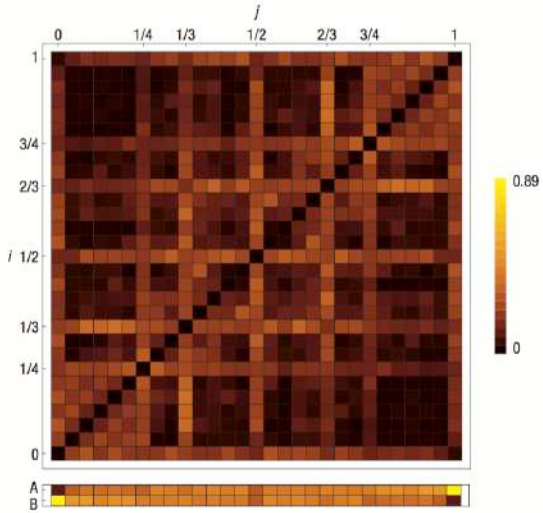


Fischer et al Predicting crystal structure by merging data mining with quantum mechanics Nature (2006) 5, 641

# ПОИСК НОВЫХ МЕТАСТАБИЛЬНЫХ АЗОТ-НАСЫЩЕННЫХ НИТРИДОВ

| | nitrides | oxides | all inorganic solids |
|---|---|---|---|
| no. of unique ICSD phases | 1253 | 13 497 | 29 902 |
| percent metastable ($T = 0$ K) | 59.8% | 56.0% | 51.6% |
| $\Delta H(E - E_{GS})$ – median | 67 meV/atom | 15.4 meV/atom | 14.9 meV/atom |
| $\Delta H(E - E_{GS})$ – 90th percentile | 190 meV/atom | 62 meV/atom | 70 meV/atom |
| median cohesive energy | −6.38 eV/atom | −6.26 eV/atom | −4.88 eV/atom |
| electronegativity | 3.02 | 3.44 | |

Stabilization of nitrogen-rich metastable nitrides

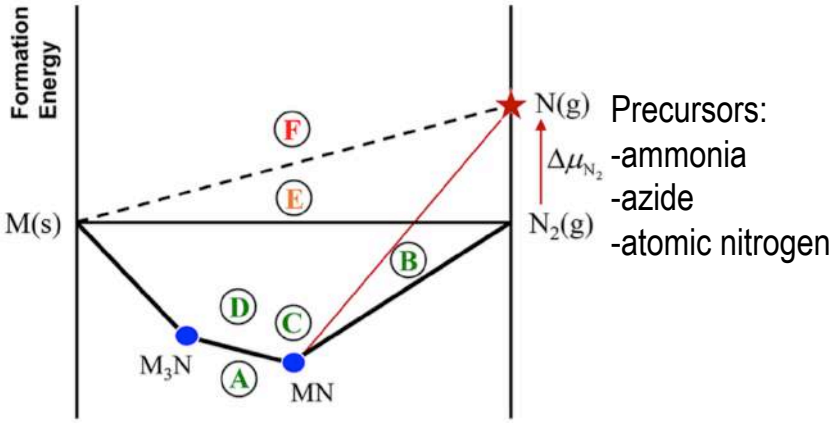


Precursors:
-ammonia
-azide
-atomic nitrogen

*Negative Formation Energy w.r.t Ambient Conditions*

- **A.** Stable Compound
- **B.** Stabilizable by Reactive Nitrogen Precursors
- **C.** Metastable Polymorph
- **D.** Metastable Phase-Separating
- **E.** Negative Formation Energy w.r.t Sputtering
- **F.** No Thermodynamic Driving Force

Probability of finding nitride with known structure from suggested candidates (TP rate)

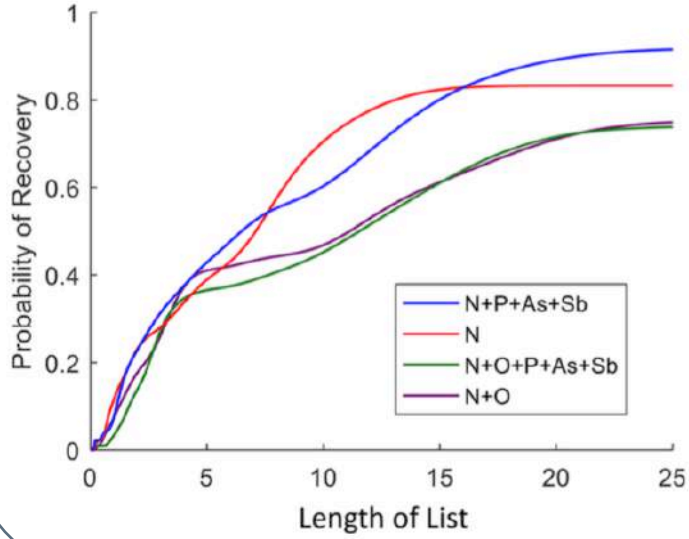


Sun et al Thermodynamic Routes to Novel Metastable Nitrogen-Rich Nitrides Chem. Mater. 2017, 29, 6936−6946

# ПОИСК НОВЫХ МЕТАСТАБИЛЬНЫХ АЗОТ-НАСЫЩЕННЫХ НИТРИДОВ

Substitution matrix for nitrides and oxides predicted by DMSP approach

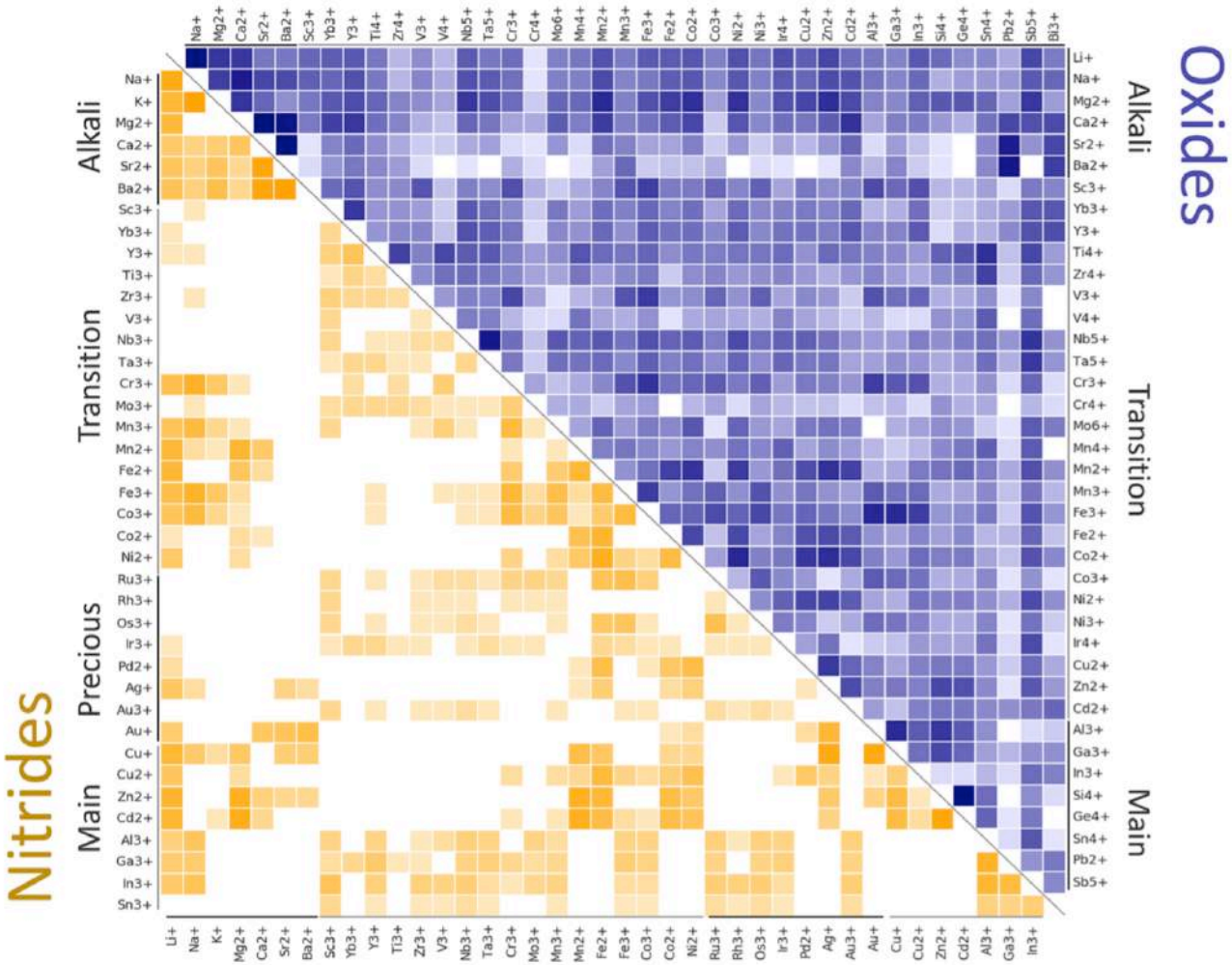


Sun et al Thermodynamic Routes to Novel Metastable Nitrogen-Rich Nitrides Chem. Mater. 2017, 29, 6936−6946

# ПОИСК НОВЫХ МЕТАСТАБИЛЬНЫХ АЗОТ-НАСЫЩЕННЫХ НИТРИДОВ

| nitride compd | prototype ICSD ID | prototype structure | space group | $E$ abv hull (eV/atom) | decomp products | pernitride | critical $\mu N_2$ (eV/atom) |
|---|---|---|---|---|---|---|---|
| $RuN_2$*[b] | 167872 | $RhN_2$ | $F\bar{4}3m$ | 0.10 | $Ru + N_2$ | N | 0.20 |
| $Nb_3N_5$ | 76460 | $Ta_3N_5$ | $Cmcm$ | 0.03 | $Nb_5N_6 + N_2$ | N | 0.20 |
| $Sn_3N_4$*[c] | 89525 | $Sn_3N_4$ | $Fd\bar{3}m$ | 0.16 | $Sn + N_2$ | N | 0.29 |
| $V_3N_4$ | 100135 | $Si_3N_4$ | $P2_1/m$ | 0.04 | $VN + N_2$ | N | 0.30 |
| $ReN_2$*[d] | 187441 | $ReN_2$ | $C2/m$ | 0.23 | $Re_3N + N_2$ | Y | 0.41 |
| $RuN_2$*[b] | 240754 | $RuN_2$ | Pmnn | 0.30 | $Ru + N_2$ | N | 0.45 |
| $PtN_2$*[e] | 166462 | $PtN_2$ | $Pa\bar{3}$ | 0.30 | $Pt + N_2$ | Y | 0.45 |
| ReN | 162871 | BN | $Cm$ | 0.16 | $Re_3N + N_2$ | N | 0.48 |
| $OsN_2$*[f] | 260545 | $OsN_2$ | $P6/mmm$ | 0.35 | $Os + N_2$ | N | 0.52 |
| $FeN_2$ | 240759 | $OsN_2$ | $Pnnm$ | 0.18 | $FeN + N_2$ | Y | 0.54 |
| $IrN_2$*[f] | 240755 | $IrN_2$ | $P2_1/c$ | 0.38 | $Ir + N_2$ | Y | 0.57 |
| $Ti_3N_4$ | 78944 | $Zr_3N_4$ | $Pnma$ | 0.09 | $TiN + N_2$ | N | 0.60 |
| $Re_3N_4$ | 156339 | $Ge_3N_4$ | $Pnma$ | 0.27 | $Re_3N + N_2$ | N | 0.64 |
| $PdN_2$*[g] | 191244 | $PdN_2$ | $Pnnm$ | 0.44 | $Pd + N_2$ | Y | 0.65 |
| $Re_3N_5$ | 95782 | $P_3N_5$ | $Imm2$ | 0.34 | $Re_3N + N_2$ | N | 0.68 |
| $Re_2N$ | 181874 | $Re_2N$ | $P6_3/mmc$ | 0.08 | $Re_3N + N_2$ | N | 0.72 |
| SbN | 162883 | BN | $P_21/c$ | 0.40 | $Sb + N_2$ | N | 0.80 |
| $Cu_2N_2$ | 60168 | MoN | $P\bar{1}$ | 0.40 | $Cu + N_2$ | Y | 0.81 |
| $CrN_2$ | 240754 | $RuN_2$ | $Pnnm$ | 0.27 | $CrN + N_2$ | Y | 0.82 |
| $Na_3N$*[h] | 421115 | $Na_3N$ | $Pm\bar{3}m$ | 0.21 | $Na + N_2$ | N | 0.84 |
| $Cr_3N_4$ | 156339 | $Ge_3N_4$ | $Pnma$ | 0.13 | $CrN + N_2$ | N | 0.92 |
| $Mn_3N_4$ | 100135 | $Si_3N_4$ | $P2_1/m$ | 0.13 | $MnN + N_2$ | N | 0.92 |
| $Mo_3N_5$ | 95782 | $P_3N_5$ | $Imm2$ | 0.22 | $MoN + N_2$ | N | 0.97 |
| $Ti_3N_4$ | 92156 | $Si_3N_4$ | $P31c$ | 0.14 | $TiN + N_2$ | N | 1.00 |
| $Cu_3N$*[I] | 53313 | $Cu_3N$ | $Pm\bar{3}m$ | 0.26 | $Cu + N_2$ | N | 1.04 |
| $Pb_3N_2$ | 91273 | $NiSr_2N_2$ | $Pnma$ | 0.42 | $Pb + N_2$ | N | 1.05 |
| $TiN_2$*[j] | N/A | $TiN_2$ | $I4/mcm$ | 0.39 | $TiN + N_2$ | N | 1.18 |
| $MoN_2$*[l] | 260549 | $OsN_2$ | $P4/mbm$ | 0.38 | $MoN + N_2$ | Y | 1.23 |
| $Pb_3N_4$ | 41952 | $C_3N_4$ | $R3m$ | 0.75 | $Pb + N_2$ | Y | 1.32 |
| $Pb_3N_2$ | 182699 | $Nb_2N_3$ | $Pnma$ | 0.54 | $Pb + N_2$ | N | 1.35 |
| $Mo_2N_3$ | 16528 | $MoNCl_3$ | $P\bar{1}$ | 0.24 | $MoN + N_2$ | N | 1.37 |
| BiN | 162876 | BN | $Pnma$ | 0.72 | $Bi + N_2$ | N | 1.44 |
| $Pd_3N_2$ | 162795 | $Ca_3N_2$ | $C2/m$ | 0.58 | $Pd + N_2$ | N | 1.46 |

Perspectives:

- Down-conversion nitride materials
- Localized surface plasmon resonance materials

Sun et al Thermodynamic Routes to Novel Metastable Nitrogen-Rich Nitrides Chem. Mater. 2017, 29, 6936−6946

# АНАЛИЗ ЛОКАЛЬНОЙ СТРУКТУРЫ МАТЕРИАЛА

# Анализ локальной структуры материала

Определение локальной структуры материала при недостаточной информативности структурного фактора (несколько кристаллографических фаз, присутствие сложных дефектов): многомерный статистический анализ координационных сфер отдельных атомов с использованием метрики между атомом и его окружением для определения структуры и симметрии

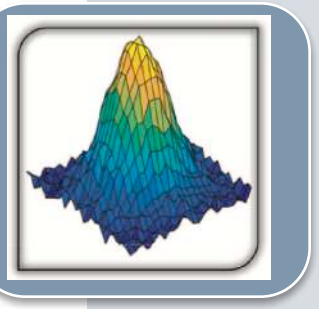

Аппроксимация формы атома при помощи идентификации репрезентативной части изображения, построение корреляционной карты

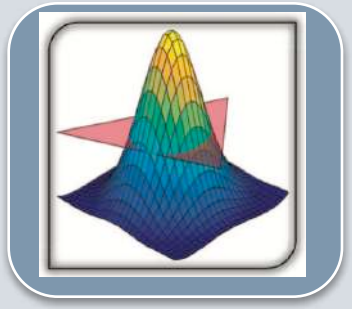

Удаление шума

Идентификация центроидов

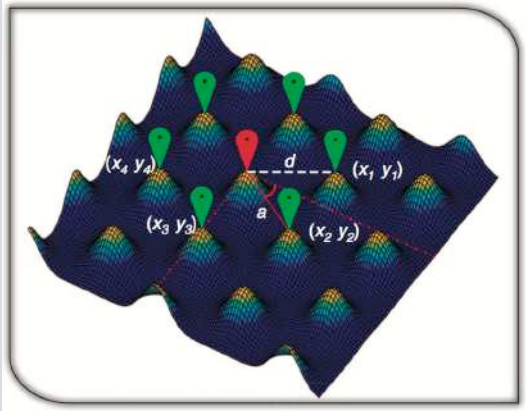


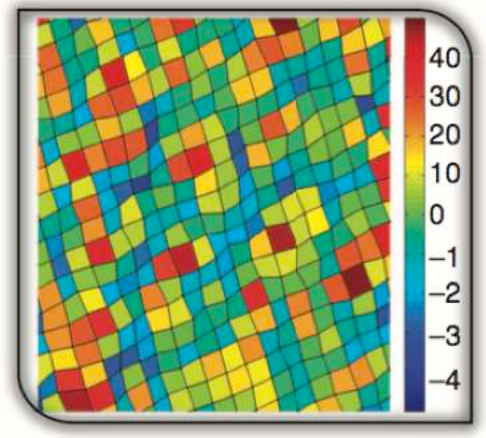


Belianinov et al Identification of phases, symmetries and defects through local crystallography Nature Communications (2015), 6, 7801

# Анализ локальной структуры материала

Two-phase Mo–V–Te–Ta oxide

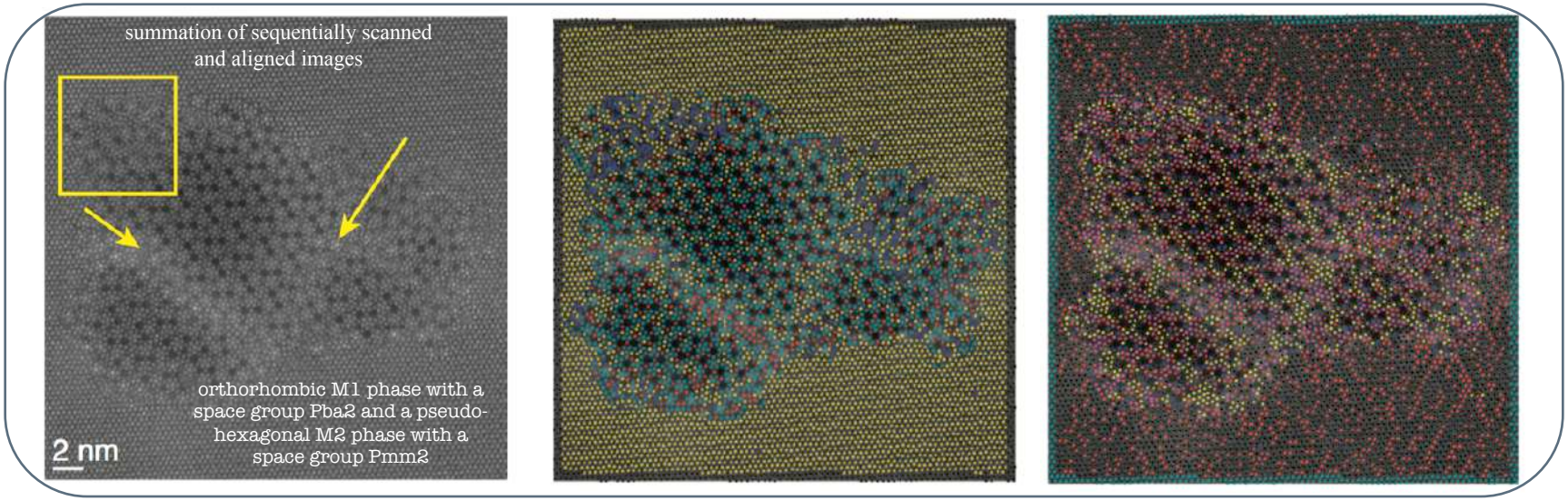


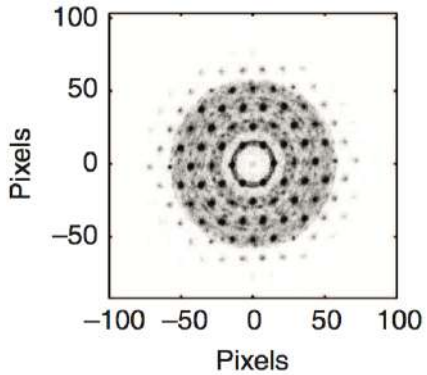


50 neighbors

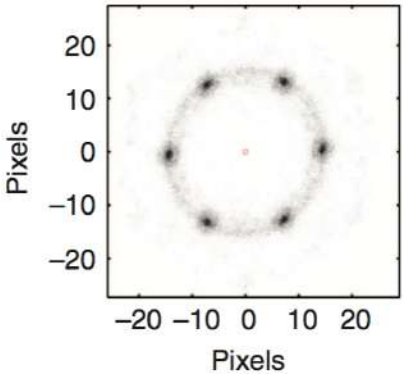


6 neighbors

Near-coordination sphere for each atom: $\mathbf{N}_i = ([x_1, y_1]..., [x_j, y_j])$

$K$-means clustering: $\arg\min_{S} \sum_{i=1}^{K} \sum_{\mathbf{x}_j \in S_i} \|\mathbf{x}_j - \mu_i\|^2$

Belianinov et al Identification of phases, symmetries and defects through local crystallography Nature Communications (2015), 6, 7801

# Анализ локальной структуры материала

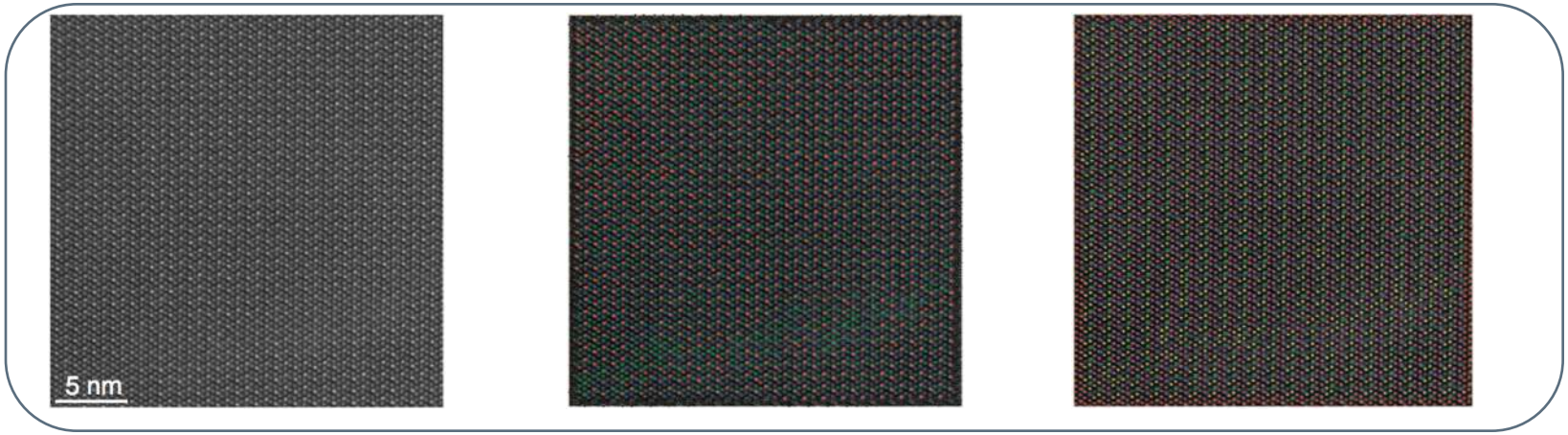


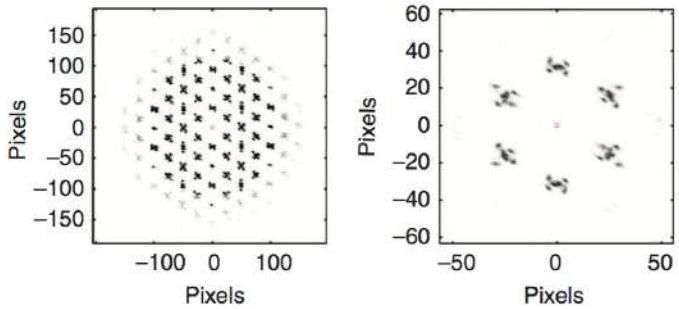


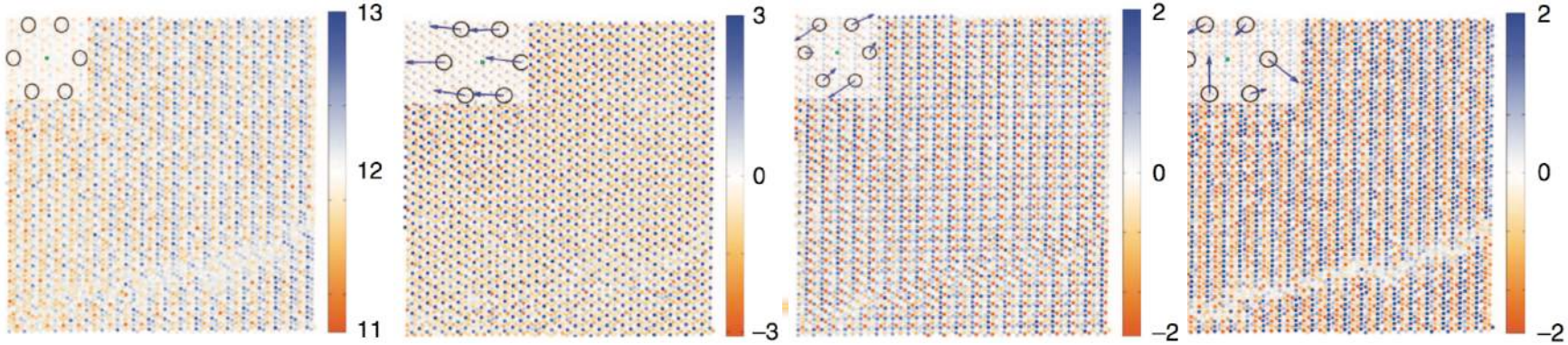


Principal Component Analysis

Belianinov et al Identification of phases, symmetries and defects through local crystallography Nature Communications (2015), 6, 7801

# АНАЛИЗ ЛОКАЛЬНОЙ СТРУКТУРЫ МАТЕРИАЛА: ИСПОЛЬЗОВАНИЕ МЕТОДОВ ГЛУБОКОГО ОБУЧЕНИЯ

Возможности:

- Анализ кристаллических решеток и структуры и типа дефектов
- Уточнение типа структуры
- Извлечение значимых структурных/химических параметров

Обучающий набор данных (искусственные данные, мимикрирующие данные STEM):

- Идеальная кристаллическая решетка
- Решетка с присутствием вакансии
- Атом-допант с большим атомным номером

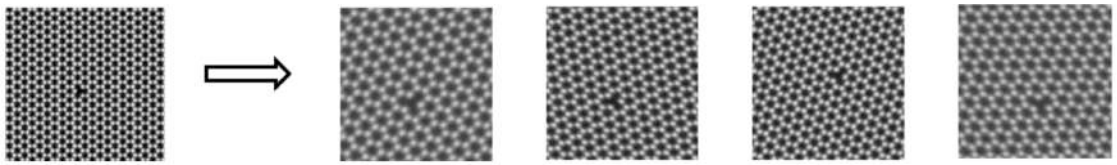

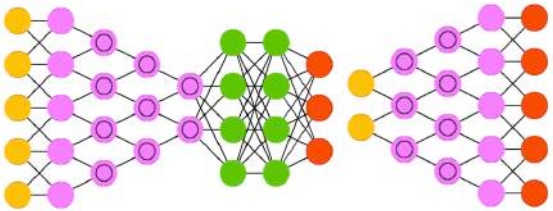

- Finding atomic positions from raw experimental data
- Pixel-wise recognition of atomic defects and lattice reconstructions
- Possible chemical structure-related interpretation of output

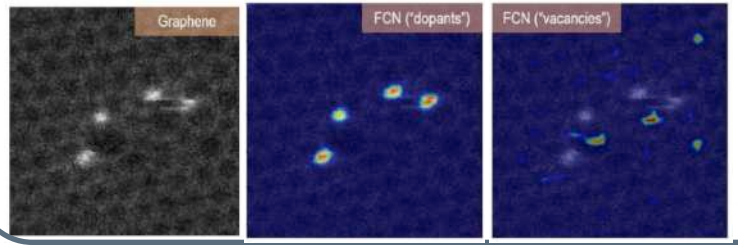


Identifying “not-seen” defects:

Stone-Wales defects in graphene

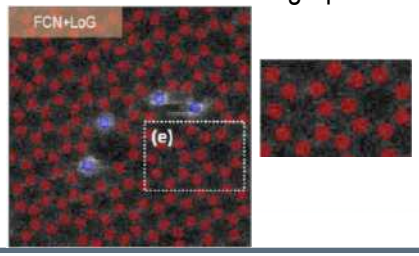


Discriminating vacancy type

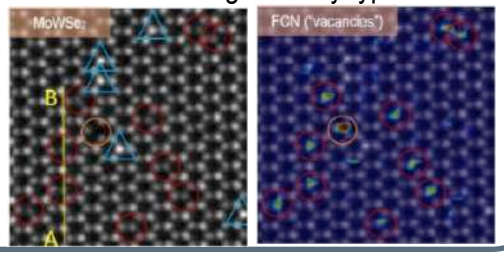


Maxim Ziatdinov et al **Deep Learning of Atomically Resolved Scanning Transmission Electron Microscopy Images: Chemical Identification and Tracking Local Transformations** *ACS Nano* **2017** *11* (12), 12742-12752

# CONVOLUTIONAL NEURAL NETWORKS

Specific characteristics:

- local connections
- shared weights
- pooling
- using many layers

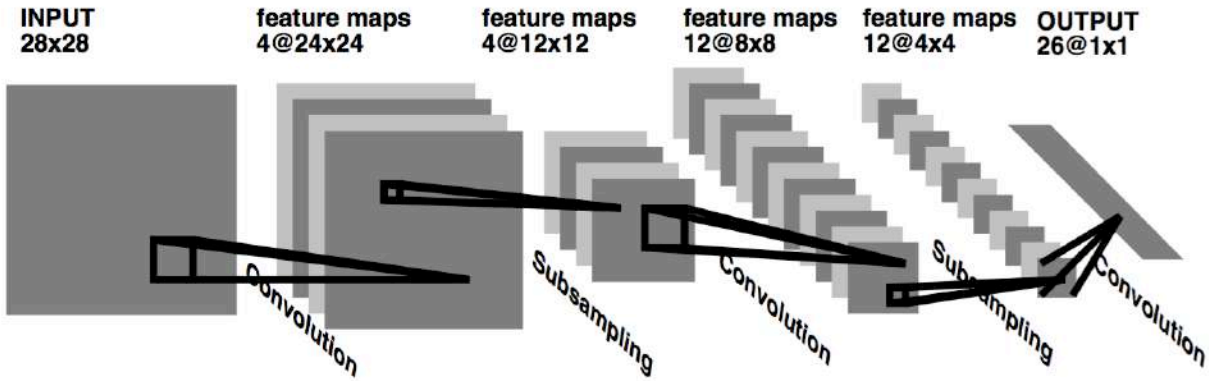


Convolution layer

Pooling

Fully connected layer

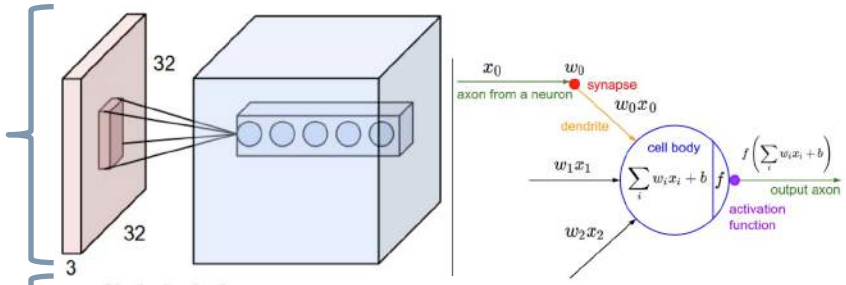


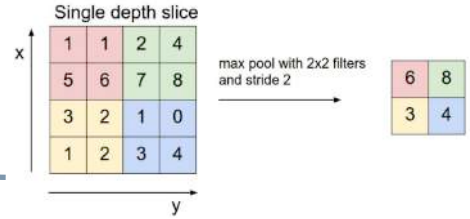


Параметры метода:

- Число фильтров
- Размер фильтров
- Шаг
- Чередование слоев

# АНАЛИЗ ЛОКАЛЬНОЙ СТРУКТУРЫ МАТЕРИАЛА: ИСПОЛЬЗОВАНИЕ МЕТОДОВ ГЛУБОКОГО ОБУЧЕНИЯ

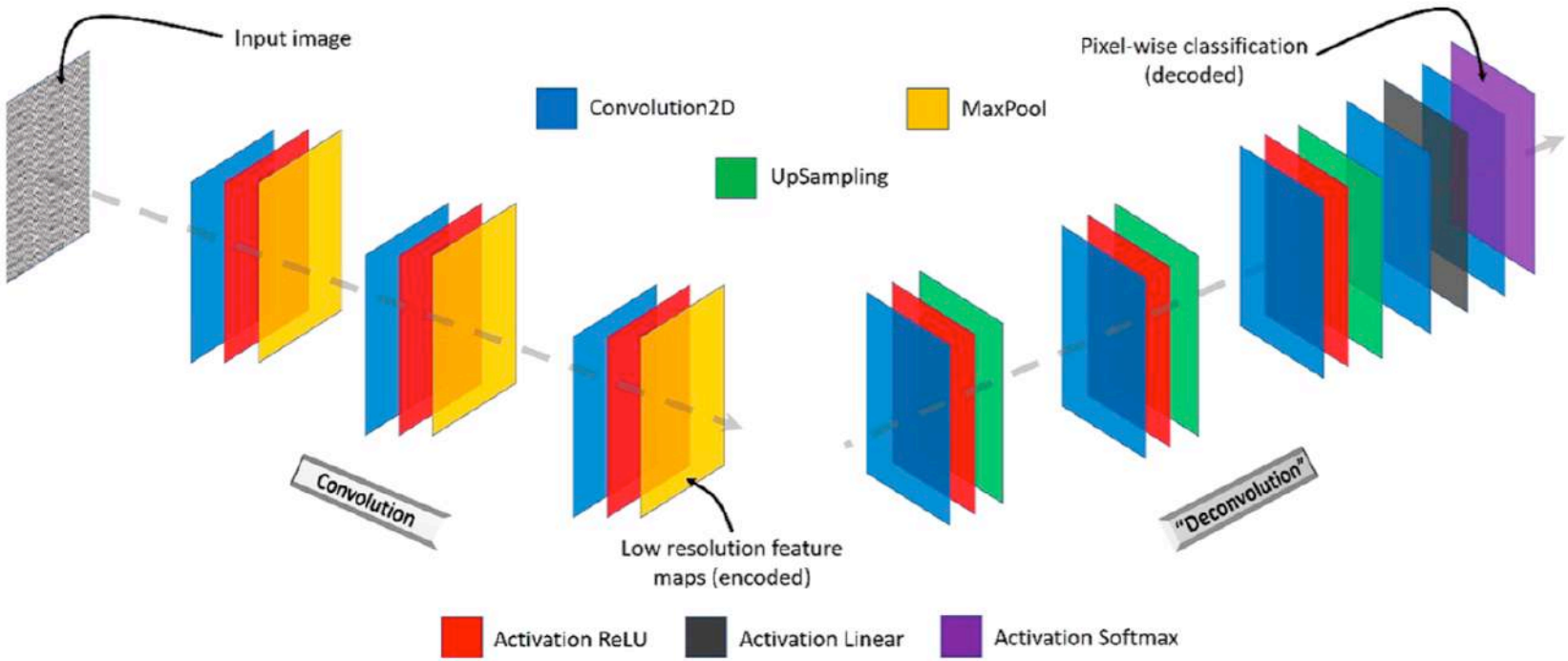


Maxim Ziatdinov et al **Deep Learning of Atomically Resolved Scanning Transmission Electron Microscopy Images: Chemical Identification and Tracking Local Transformations** *ACS Nano* **2017** *11* (12), 12742-12752

# АНАЛИЗ ЛОКАЛЬНОЙ СТРУКТУРЫ МАТЕРИАЛА: ИСПОЛЬЗОВАНИЕ МЕТОДОВ ГЛУБОКОГО ОБУЧЕНИЯ

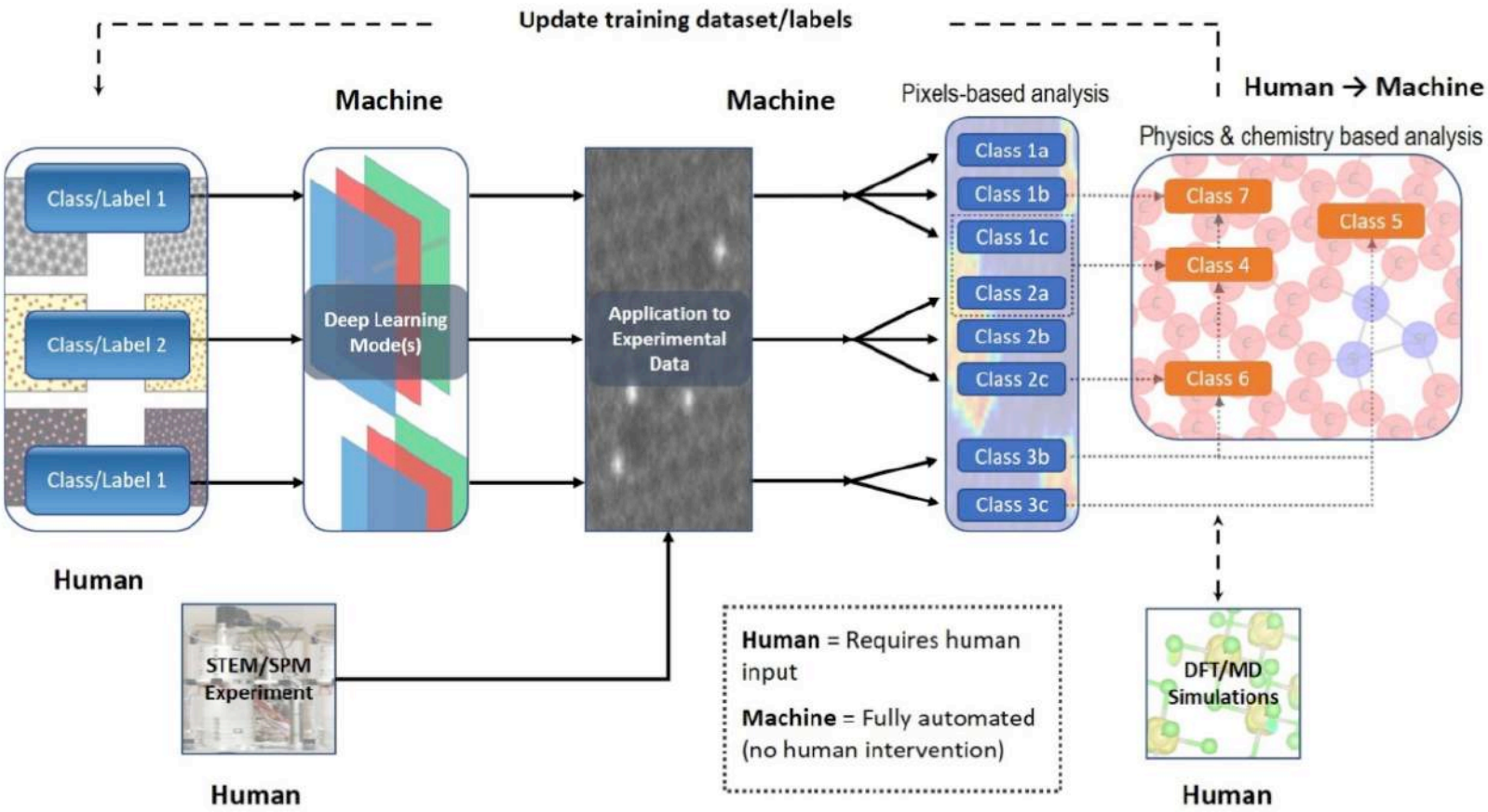


Maxim Ziatdinov et al **Deep Learning of Atomically Resolved Scanning Transmission Electron Microscopy Images: Chemical Identification and Tracking Local Transformations** *ACS Nano* **2017** *11* (12), 12742-12752

# АНАЛИЗ ПРОЦЕССОВ, ПРОИСХОДЯЩИХ НА ИНТЕРФЕЙСАХ: МЕЖЗЁРЕННЫЕ ГРАНИЦЫ

# PHASE BEHAVIOR OF INTERFACES: COMPLEXIONS

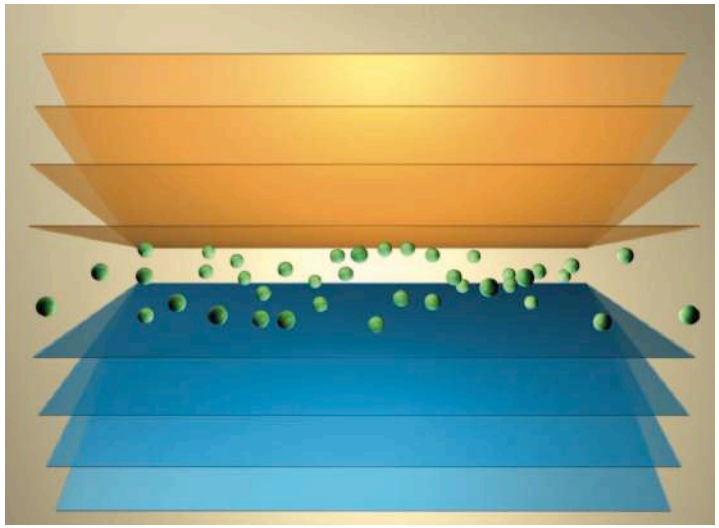

Grain boundary (GB) can be viewed as interface-stabilized “complexion” phase that can be formed between different crystals within a material and that are chemically and structurally distinct from any bulk phases and can be chemically and structurally inhomogenious

Nanoscale interface structures are equilibrium phases that obey thermodynamic rules analogous to those of bulk phases

A number of unexplained observations concerned:

- abnormal grain growth
- deliberate incorporation of certain atomic elements into grain boundaries can drastically change the materials properties

# THE IMPORTANCE OF GRAIN BOUNDARY COMPLEXIONS IN AFFECTING PHYSICAL PROPERTIES

Some effects of complexions on diffusional transport and physical properties

- Non-Arrhenius enhancement of diffusional transport limited processes such as sintering and grain growth, unascertained impact on ion diffusion processes
- Activated sintering process
- Coarse grain structure obtained after prolonged annealing at high tº on average exhibit different complexions -> complex unexpected materials behavior
- The presence of localized phonon modes as a result of layering transitions may lead to modified localized interfacial vibrational modes

# THE PHASE BEHAVIOR OF INTERFACES: MICROWAVE DIELECTRIC PROPERTIES

Aeschynites/Euxenites

$La_{1-x}Ce_xTiNbO6$

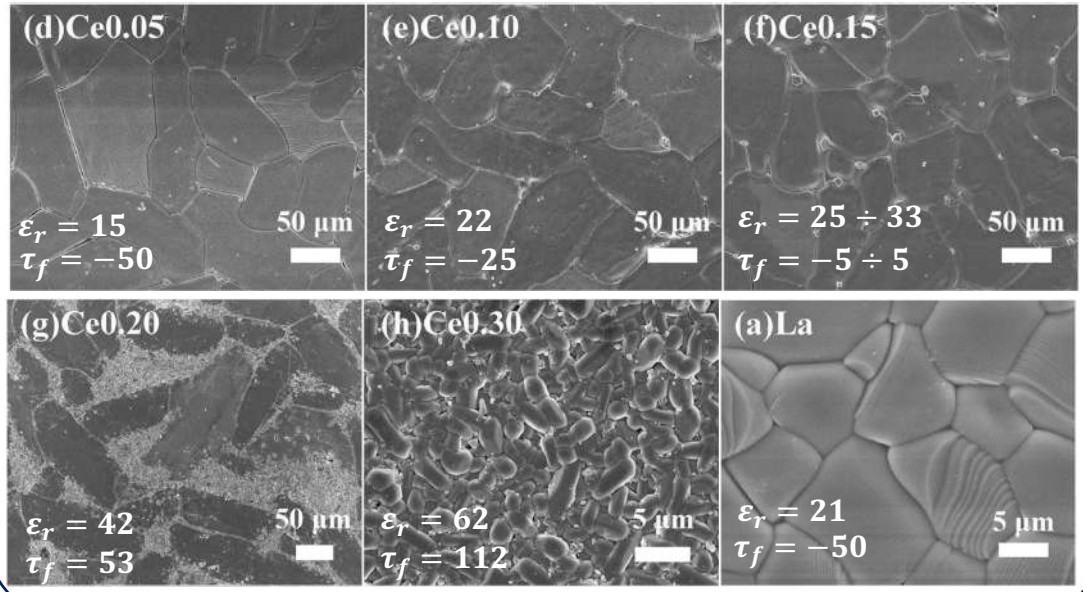


Rietveld refinement plots of $La_{0.85}Ce_{0.15}TiNbO6$

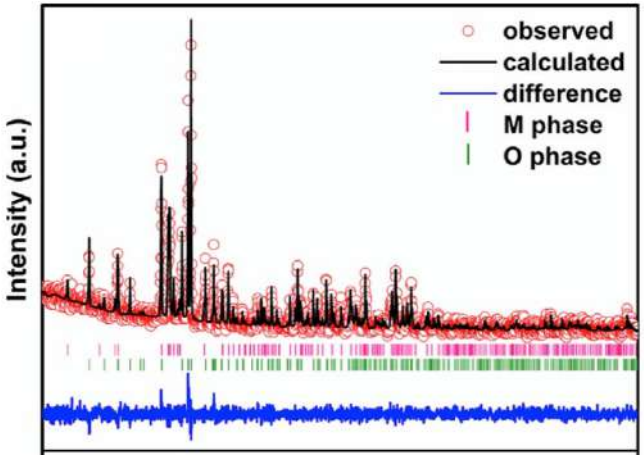


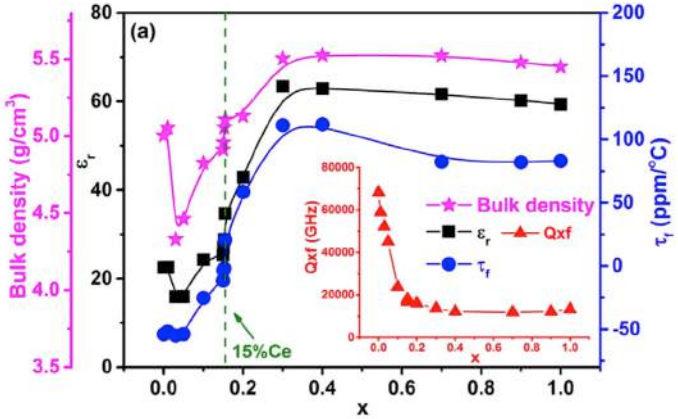


Raman spectra of $La_{1-x}Ce_xTiNbO6$

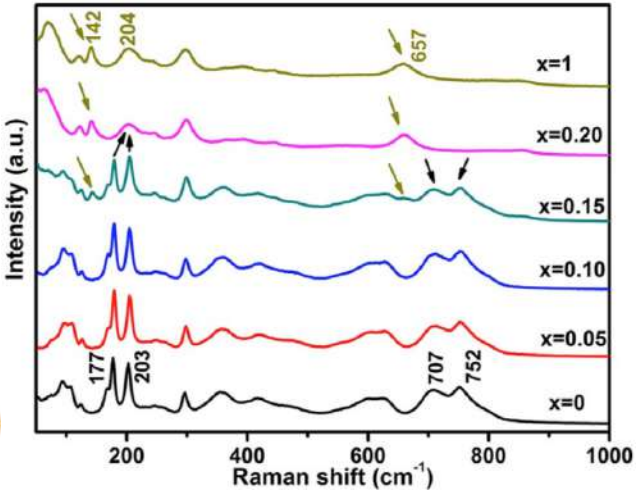


Zhang et al Phase structural transition and microwave dielectric properties in isovalently substituted $La_{1-x}Ln_xTiNbO_6$ (Ln=Ce, Sm) ceramics Ceramics International 43 (2017) 7065–7072

# ANALYSIS OF INTERFACE PROCESSES IN CERAMICS: GRAIN BOUNDARIES

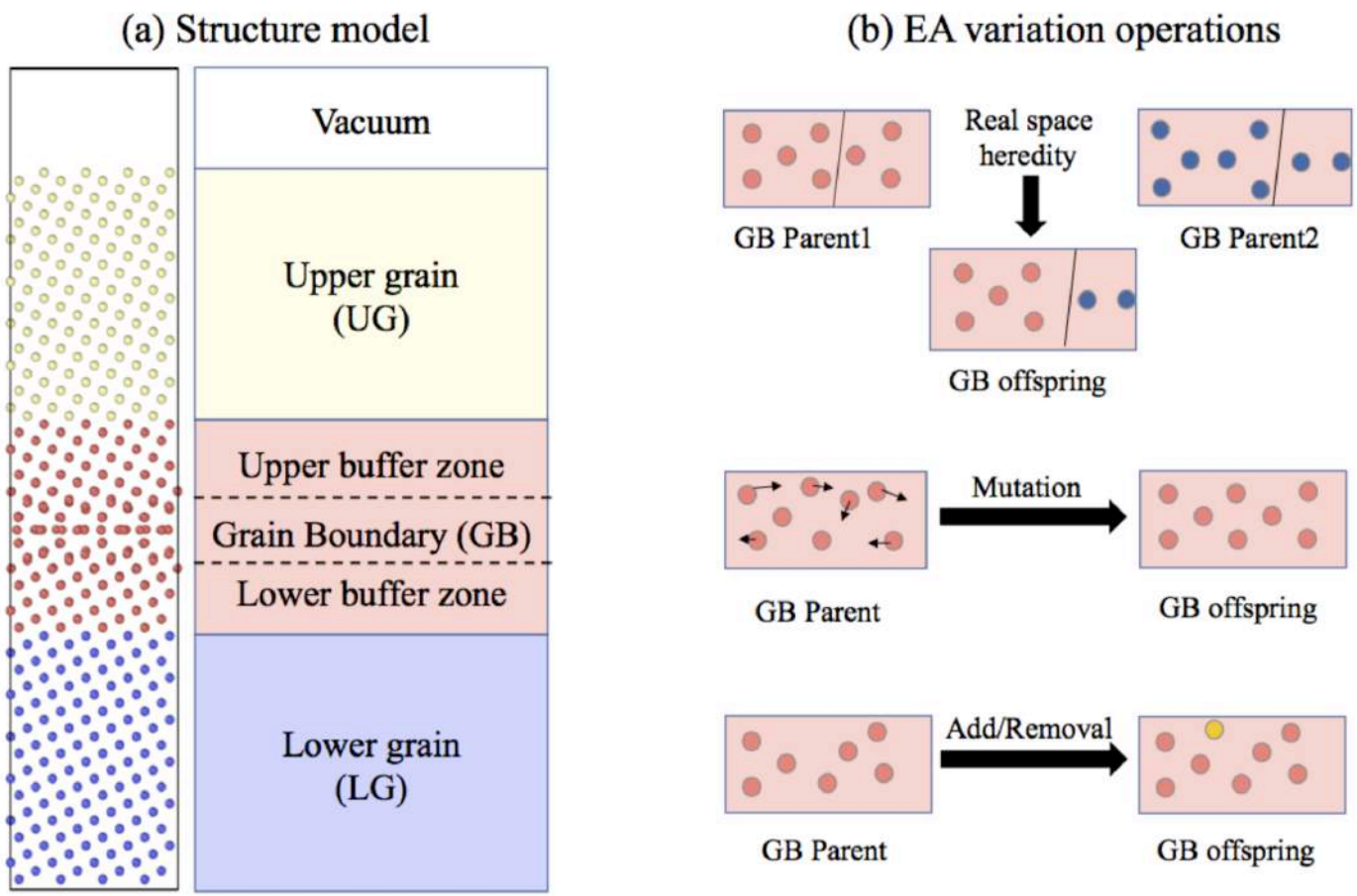

# ANALYSIS OF INTERFACE PROCESSES IN CERAMICS: GRAIN BOUNDARIES (GB)

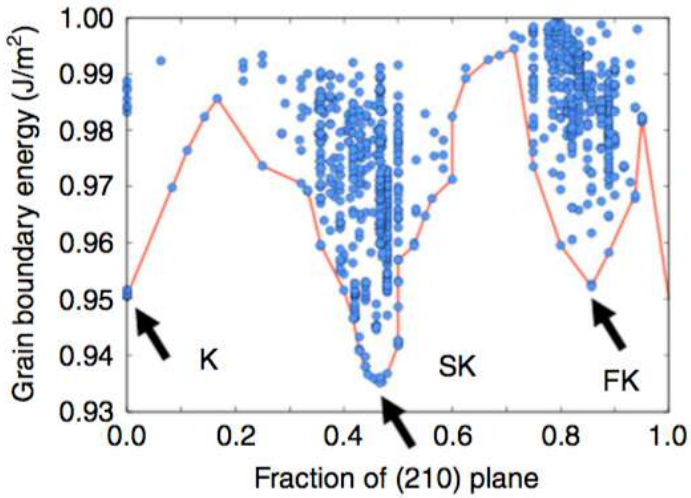


Identifying the number and type of grain boundary phases by virtue of clustering algorithms

- Descriptors
  - thermodynamics-based
    - excess volume per unit area
    - GB stress tensor
    - number of atoms
  - structural features
    - Steinhardt order parameters

GBs distinguished

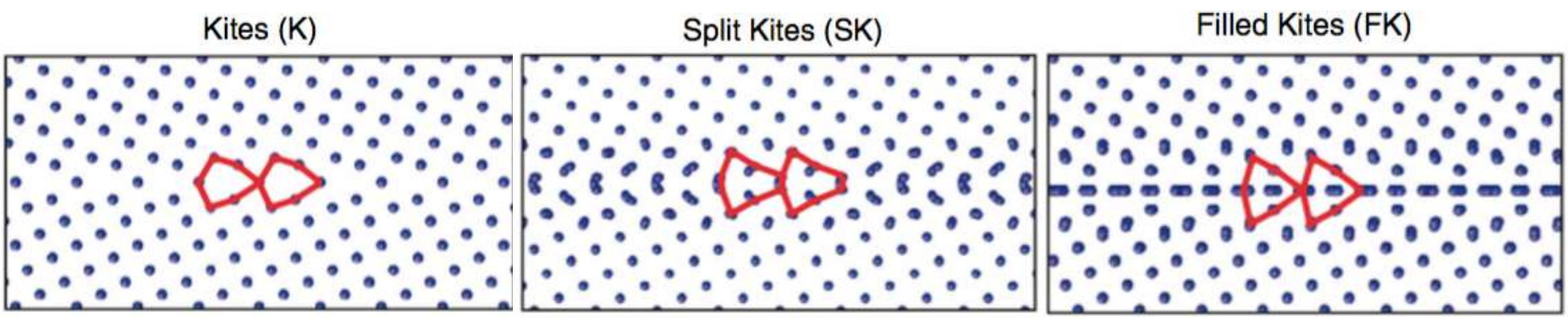

# MATERIALS SYNTHESIS DETAILS AS PARAMETERS UNRAVELING COMPOSITION-STRUCTURE-PROPERTY RELATIONSHIPS

# VIRTUAL SCREENING OF INORGANIC MATERIALS SYNTHESIS PARAMETERS WITH DEEP LEARNING

Descriptors:
processing (synthesis) information – sintering and calcination temperature and time, method of synthesis, solvent

Tasks:
- SrTiO3/BaTiO3 synthesis details discriminating
- MnO2 polymorph elucidation

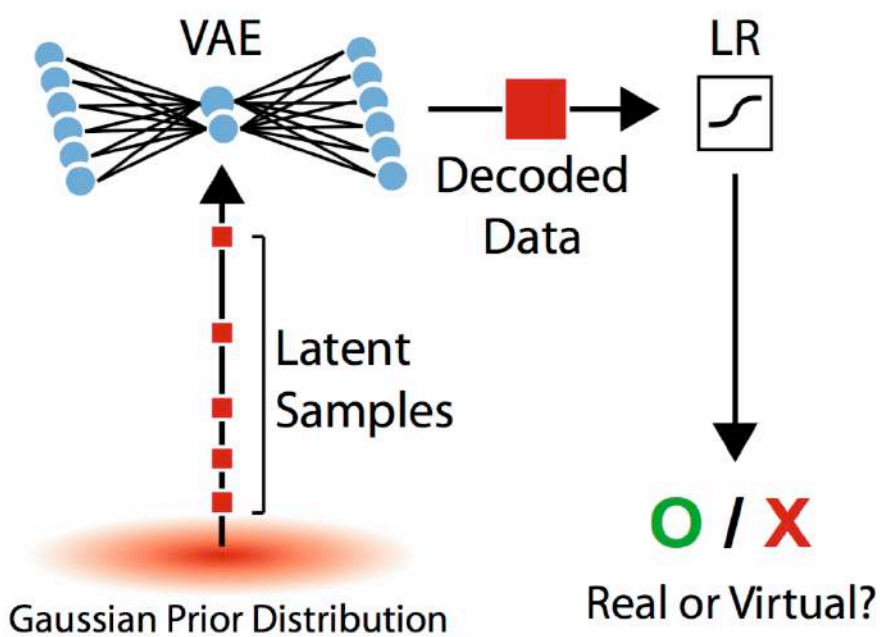


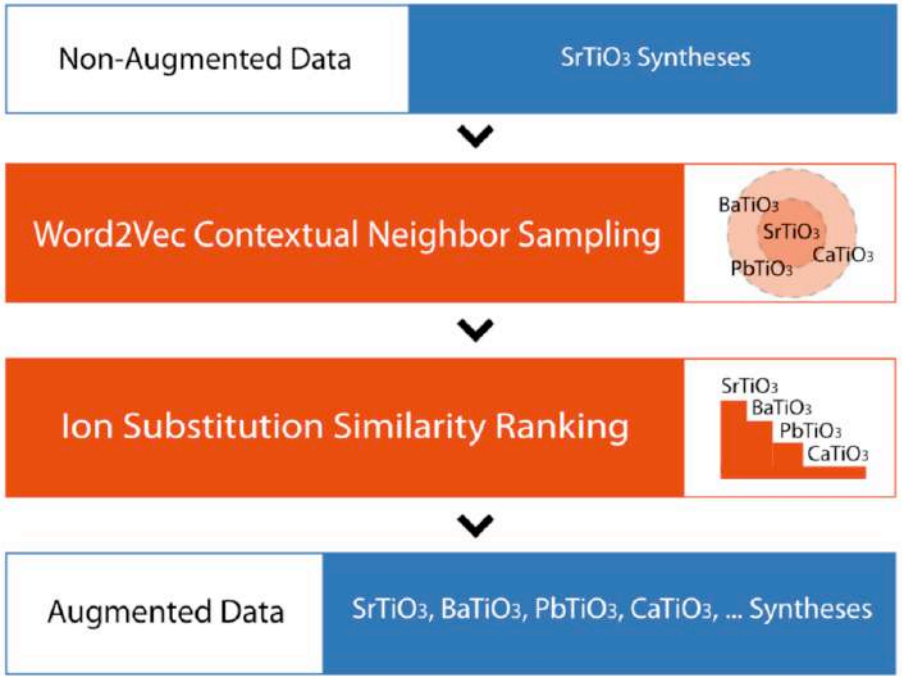


Kim et al npj Computational Materials (2017) 53

# VIRTUAL SCREENING OF INORGANIC MATERIALS SYNTHESIS PARAMETERS WITH DEEP LEARNING

Loss function:

$$\mathcal{L}(x, \hat{x}) + \sum_j KL\left(q_j(z|x) \,||\, p(z)\right)$$

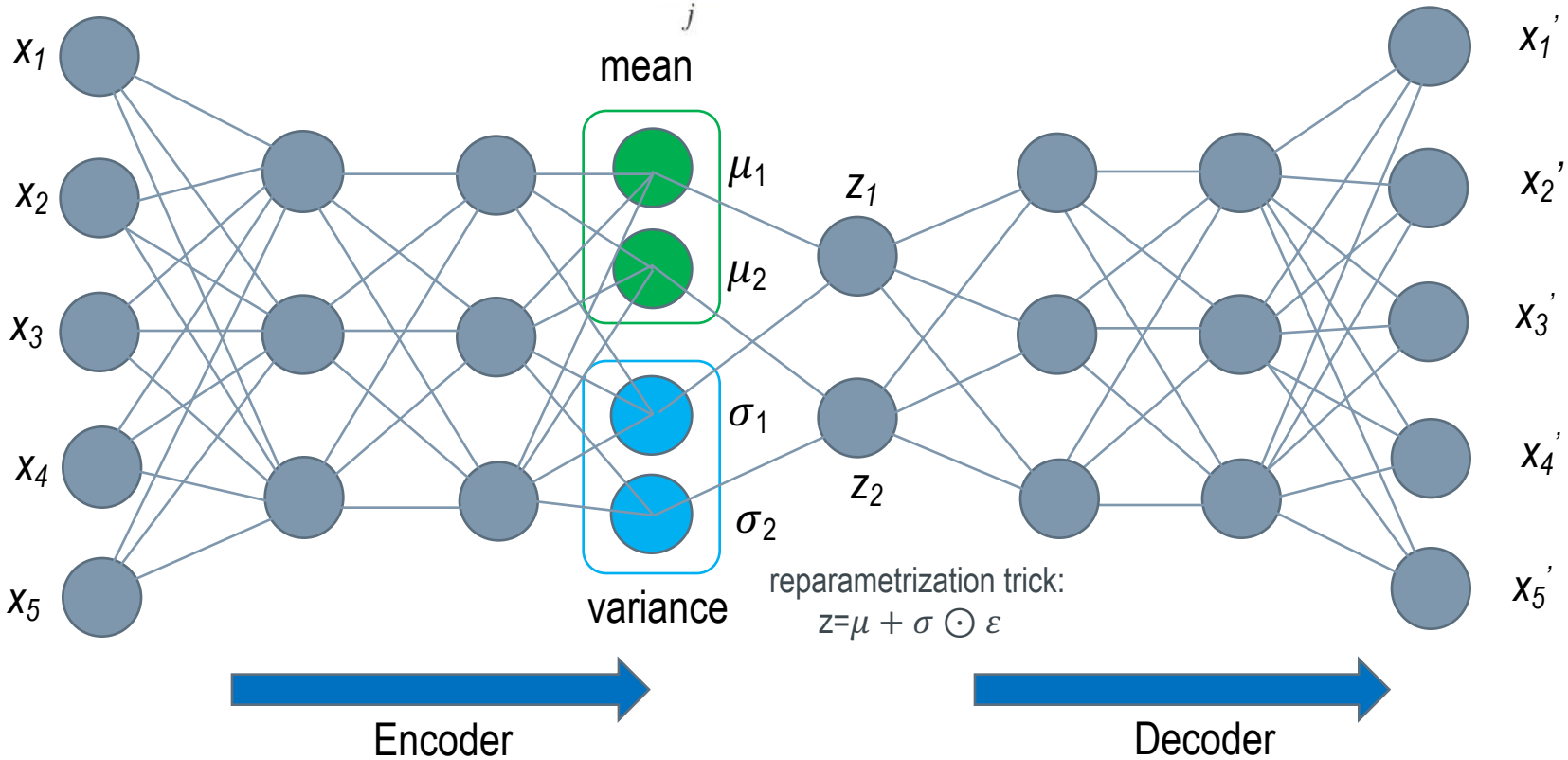


Kim et al npj Computational Materials (2017) 53